A Hybrid Proximity Effect Correction Method based on Separation of Forward-/Back-Scattering and Cumulative Distribution Function

Jiaxin Chen[a], Haojie Zhao[a], Siyuan Zhang[a], Yujie Yang[a], Wenze Yao[a],
Xin Zhang[b], Pinghui Mo[b], Jie Liu*[b]

[a]College of Electrical and Information Engineering, Hunan University, Changsha, P.R. China;
[b]College of Integrated Circuits, Hunan University, Changsha, P.R. China

ABSTRACT

Efficient and accurate proximity effect correction (PEC) is essential for electron beam lithography (EBL) applications. Here we present an efficient PEC method by combining cumulative distribution function (CDF) and separation of forward and back-scattering. Dose and shape hybrid corrections are used together to further enhance PEC accuracy. Compared to the traditional pixelation algorithms, the proposed method can enhance modeling efficiency by three orders of magnitude, while keeping the edge placement error (EPE) below one nanometer, in our testbench calculations. The proposed method might be useful in large-scale mask data preparation (MDP) and direct-write EBL applications.

Keywords: Electron Beam Lithography, Mask Data Preparation, Proximity Effect Correction, Cumulative Distribution Function

1. INTRODUCTION

Electron beam lithography (EBL) is a high-resolution maskless direct-write lithography for micro-nano patterning. Proximity effect (PE) may reduce the actual exposure resolution of EBL[1]. To ensure fabrication quality, proximity effect correction (PEC) is essential[2-6]. However, the traditional pixel-level PEC method is extremely time-consuming and memory-consuming. To solve this problem, we propose an efficient hybrid correction method in which the time-/memory-consuming vary linearly with the layout size. Compared with the traditional pixel-level PEC method, the efficiency of the proposed method is improved by more than 3 orders of magnitude.

The proposed hybrid PEC method computes the energy deposition values by accumulation of the forward-/back-scattering energy deposition values. The forward-scattering deposition values are calculated by constructing the cumulative distribution function (CDF) table and R-tree. The back-scattering energy deposition values are calculated by fast Fourier transform (FFT) convolution of large meshes and spline interpolation. After PE simulation, the final high-quality exposure layout is achieved through dose correction and shape correction. The accuracy and effectiveness of the proposed method implemented in HNU-EBL (http://www.ebeam.com.cn)[7-10] which have been verified by EBL experiments. Section 2 provides a detailed description of the proposed method. Section 3 introduces the dataset source used in our experiment. Section 4 discusses the performance of the proposed method. Section 5 presents a summary.

2. METHODOLOGY

In Section 2A. Hybrid correction, the hybrid correction method including dose correction and shape correction is presented; In Section 2B. Forward-/back-scattering, the theory of the forward-/back-scattering separation is discussed. In Section 2C. Forward-scattering, the steps of calculating forward-scattering energy deposition values by CDF are introduced. In Section 2D. Back-scattering, the steps of calculating back-scattering energy deposition values by FFT are introduced. In Section 2E. EPE, the calculation method of EPE is briefly described.

Figure 1(a) shows the schematic calculation flow of the proposed method. After fracturing, the forward-/back-scattering separation method (Figure 1(b)) is applied to computing the energy deposition. A hybrid PEC method is implemented for continuous optimization. Finally, the calculation results, which satisfy the requirements of edge placement errors (EPE), are obtained.

*jie_liu@hnu.edu.cn; http://www.ebeam.com.cn/

Eighth International Workshop on Advanced Patterning Solutions (IWAPS 2024),
edited by Yayi Wei, Tianchun Ye, Proc. of SPIE Vol. 13423, 134230X
 · 0277-786X · doi: 10.1117/12.3052975

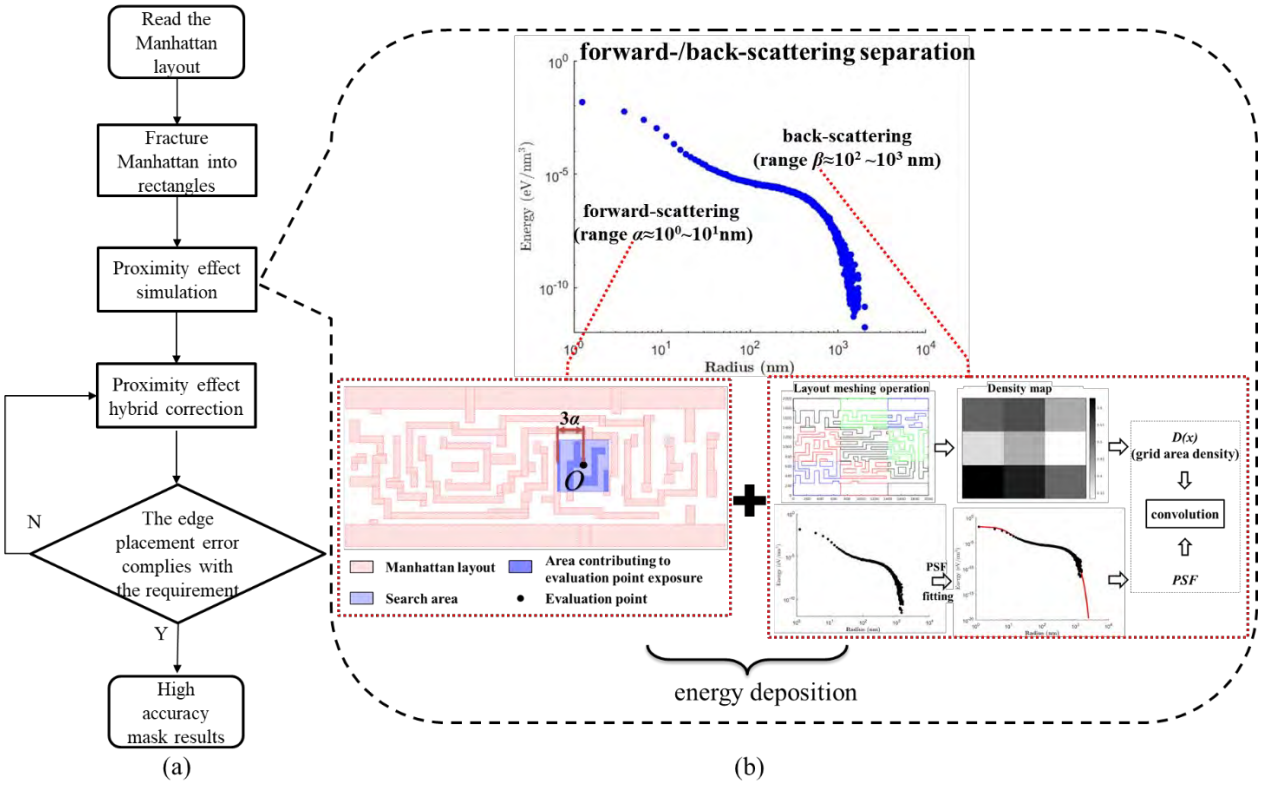

Figure 1. (a) The calculation flow of the proposed method. (b) Schematic diagram of forward-/back-scattering separation.

A. Hybrid correction

In EBL exposure, electrons will collide with nuclei and electrons of the photoresist and substrate. During the collision process, the electrons lose energy while changing the motion trajectory, resulting in the distribution of energy deposition density in the photoresist that does not meet the expectations, and eventually the exposure effect is seriously distorted relative to the target layout[1]. PEC must be carried out to ensure the accuracy of EBL. The proposed PEC method includes two modules: dose correction and shape correction.

The dose correction method[11] mainly consists of the following four steps:

***Step* (1)** Target layout preprocessing. The gap-based heuristic ray-selective splitting algorithm[12] is used to split the polygon into multiple non-overlapping rectangles and reduce the number of rectangles as much as possible. However, electron forward-scattering results in PE comparable to the critical dimension (CD) of the mask[13], which must be considered during fracturing. Therefore, the preliminary fracturing results need to be further processed.

In the process of PEC, it is essential to correctly process the polygon edges. At the interior of the polygon, for positive photoresist (such as PMMA), it is only necessary for the energy deposition density to exceed a certain threshold. However, for the edge of the polygon, we pursue high contrast, such that the change of energy deposition density at the edge looks like a step function. Hence, we attach greater significance to the exposure dose on the edge of the polygon.

According to the preset minimum rectangle size m and maximum rectangle size M, the initial fracturing effect is divided from the edge to the interior, so that the rectangle size closer to the edge of the polygon is smaller, and the rectangle size in the center of the polygon is larger. For the internal rectangle, the entire rectangle is represented by the value of the energy deposition density at the center of the rectangle. For edge rectangles, the entire rectangle is represented by the midpoint of the edge where the rectangle intersects the polygon (Figure 2).

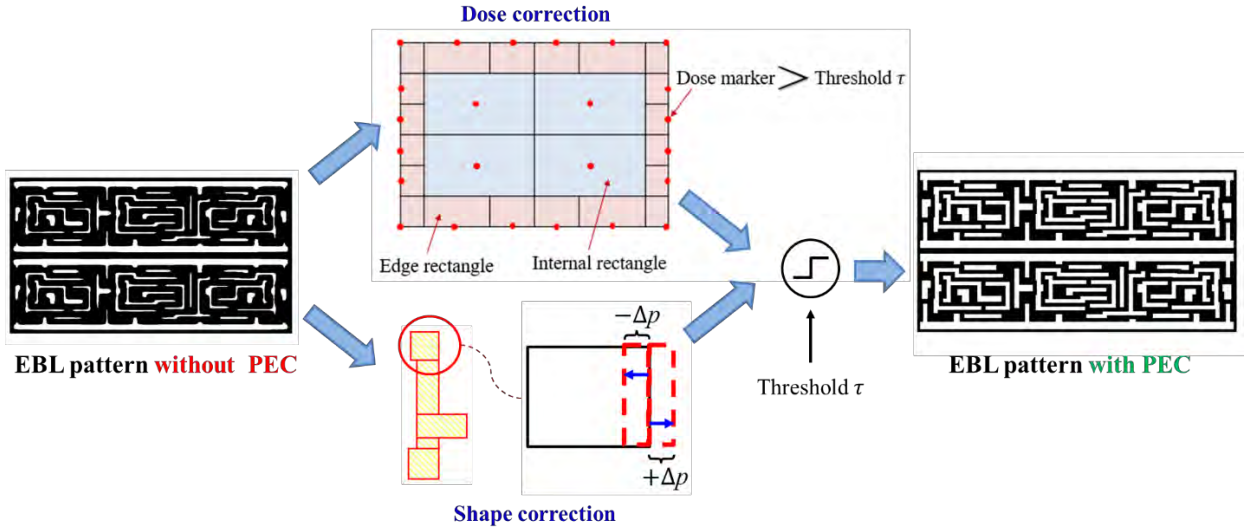

Figure 2. Schematic diagram of the proposed hybrid correction.

***Step* (2)** Calculate the energy deposition density. Dose correction adjust the exposure dose for the entire rectangle area. Therefore, the energy deposition density value of the evaluation point can effectively represent the entire rectangle region.

***Step* (3)** Dose correction. The edge rectangle makes the energy deposition density of the polygon edge tend to the development threshold during iteration, while the dose iteration of the internal rectangle tends to make the energy deposition density of the polygon internal tend to be uniform.

***Step* (4)** Repeat ***steps* (2) ~ (3)** until the iterations number reaches the preset maximum number or EPE meets the requirements.

The shape correction method[11] mainly includes the following five steps:

***Step* (1)** Traverse the polygon for shape correction. As shown in Figure 2, for the edge rectangles, we only consider two possible adjustments, that is, moving the rectangle edge by $+\Delta p$ or $-\Delta p$, where p is the offset, usually taking 1nm. Due to the limited adjustment and the minor range of forward-scattering influence, a minor adjustment of one polygon edge will have a minor influence on other polygons.

***Step* (2)** Calculate the cost function. To measure the gap between the exposure layout and the target layout, the cost function

$$cost = \sum_{p(x,y)\in P_{fail}} |E(x,y) - \tau| \quad (1)$$

needs to be defined, expressed as the accumulated absolute difference between the energy deposition density $E(x,y)$ of the failed pixel P_{fail} and the development threshold τ. If the cost function is less than the threshold, it indicates that the polygon has met the lithography requirements, and no further adjustment is required. If the cost function is greater than the threshold, shape adjustment is needed to optimize the exposure layout.

***Step* (3)** Calculate the shape adjustment score. To determine which adjustment mode optimizes the effect better, we define

$$score = cost_{n+1} - cost_n \quad (2)$$

where $cost_{n+1}$ is the cost function value after the $n+1$ shape adjustment, and $cost_n$ is the cost function value after the n shape adjustment, $score$ is the change of the cost function value before and after edge adjustment.

***Step* (4)** Greedy acceptance of shape adjustments. First, sort all edge moves in descending order of their score. Next, iterate through the sorted list of edge movement and start accepting cost reduction movement. At the same time, any other edge within a certain range of the moving edge is not allowed to move in the current iteration. Avoid a set of shape edge moves that cancel each other out in subsequent iterations.

***Step* (5)** Iterate ***steps* (1) ~ (4)** until the cost function is less than the threshold or the maximum number of iterations is reached.

B. Forward-/back-scattering separation

High-performance PE simulation calculation is the basis of accurate and efficient PEC. PE simulation can be obtained by convolving the layout incident dose with the point spread function (PSF) fitted with electron scattering. The PSF is in the form of double-Gaussian as

$$f(r) = \frac{K}{\pi(1+\eta)}\left[\frac{1}{\alpha^2}\exp\left(-\frac{r^2}{\alpha^2}\right) + \frac{\eta}{\beta^2}\exp\left(-\frac{r^2}{\beta^2}\right)\right] \tag{3}$$

where r is the distance between the target position and the electron beam incident position, α represents the characteristic half-width of the forward-scattering distribution, β represents the characteristic half-width of the back-scattering distribution, η represents the ratio of the two scattering energies, and K is a constant.

An important physical fact is that the area affected by forward-scattering is small, while the area affected by back-scattering is large. In PSF, the forward-scattering parameter α is generally in the order of 10 nm, but the back-scattering parameter β is generally in the range of 1μm~50μm. The PSF parameters are selected as α=9.8 nm, β=1826.9 nm, η=0.326, K=1. The difference in the range of the forward-/back-scattering influence is hundreds or thousands of times, which implies that different calculation schemes can be used to evaluate the forward-/back-scattering influence on the EBL exposure[4-6, 14, 15].

The Gaussian term represented by the forward-scattering parameter α, which is only a few nanometers long, decays rapidly, and only has a significant impact on the energy deposition density at very close distances. This suggests that when calculating the energy deposition density at a certain exposure point, we could only consider the forward-scattering influence in a certain region around the exposure point.

However, the back-scattering parameter β is large, which means that the Gaussian term representing back-scattering in PSF decays slowly and the curve is flat. Therefore, it can be considered that, within a certain range, the unit dose exposure influence at position $\boldsymbol{r'}$ on the energy deposition density at position $\boldsymbol{r}$ remains unchanged, which indicates that when back-scattering is calculated alone, larger uniform grids can be used to reduce the amount of data.

In fact, PE can be numerically divided into two parts with sharp and fast attenuation and flat and slow attenuation, as shown in Figure 1(b). Therefore, we do not need to be too concerned about the analytical form of PSF, while can consider it as a combination of forward-scattering and back-scattering.

C. Forward-scattering calculation

The forward-scattering energy deposition simulation method mainly consists of three steps:

***Step* (1)** Construct the CDF Rectangle (CDFR) table. CDF can be used to calculate the effective exposure dose produced by a rectangle beam spot on the surrounding area[16-18]. The effective exposure dose of any rectangle on any point in the layout can be quickly and effectively obtained. To quickly calculate the forward-scattering energy deposition influence at any location by the surrounding exposure region, we need to build a CDFR table.

The energy deposition intensity of forward-scattering is

$$\begin{aligned} E(i,j) &= \frac{K}{\pi(1+\eta)}\iint \frac{1}{\alpha^2}\exp\left(-\frac{r^2}{\alpha^2}\right)dr = \frac{K}{\pi(1+\eta)}\int_{x_1}^{x_2}\int_{y_1}^{y_2}\frac{1}{\alpha^2}\exp\left(-\frac{(x-i)^2+(y-j)^2}{\alpha^2}\right)dxdy \\ &= \frac{K}{\pi(1+\eta)}\int_{x_1-i}^{x_2-i}\frac{1}{\frac{\sqrt{2\pi}\alpha}{\sqrt{2}}}\exp\left(-\frac{x^2}{2\left(\frac{\alpha}{\sqrt{2}}\right)^2}\right)dx\int_{y_1-j}^{y_2-j}\frac{1}{\frac{\sqrt{2\pi}\alpha}{\sqrt{2}}}\exp\left(-\frac{y^2}{2\left(\frac{\alpha}{\sqrt{2}}\right)^2}\right)dy \end{aligned} \tag{4}$$

where $E(i,j)$ represents the forward-scattering energy deposition intensity generated by exposure at any position (i,j) of a rectangle region with (x_1,y_1) as the lower left vertices and (x_2,y_2) as the upper right vertices. Using the formula

$$\begin{cases} u = \frac{\sqrt{2}x}{\alpha} \\ v = \frac{\sqrt{2}y}{\alpha} \end{cases} \tag{5}$$

we have

$$E(i,j) = \frac{K}{(1+\eta)} \int_{\sqrt{2}(x_1-i)/\alpha}^{\sqrt{2}(x_2-i)/\alpha} \frac{1}{\sqrt{2\pi}} \exp\left(-\frac{u^2}{2}\right) du \int_{\sqrt{2}(y_1-j)/\alpha}^{\sqrt{2}(y_2-j)/\alpha} \frac{1}{\sqrt{2\pi}} \exp\left(-\frac{v^2}{2}\right) dv$$
$$= \frac{K}{(1+\eta)} \left[\Phi\left(\frac{\sqrt{2}(x_2-i)}{\alpha}\right) - \Phi\left(\frac{\sqrt{2}(x_1-i)}{\alpha}\right)\right] \left[\Phi\left(\frac{\sqrt{2}(y_2-j)}{\alpha}\right) - \Phi\left(\frac{\sqrt{2}(y_1-j)}{\alpha}\right)\right] \quad (6)$$

where $\Phi(\cdot)$ is expressed as the CDF of the standard normal distribution. According to the analysis of formulas (1) ~ (3), $CDFR(i,j)$ can be written as

$$CDFR(i,j) = \frac{K}{(1+\eta)} \left[\Phi\left(\frac{\sqrt{2}i}{\alpha}\right) - \Phi(0)\right] \left[\Phi\left(\frac{\sqrt{2}j}{\alpha}\right) - \Phi(0)\right] \quad (7)$$

where $CDFR(i,j)$ is defined as the forward-scattering influence of the rectangle region on the origin when unit incident dose is applied to the rectangle $[0,i] \times [0,j]$.

As shown in Figure 3, the coordinates of the rectangle and the evaluation point can be linearly transformed by taking the evaluation point (x,y) as the origin. Thus, the energy deposition

$$E(i,j) = CDFR(x_2,y_2) - CDFR(x_1,y_2) - CDFR(x_2,y_1) + CDFR(x_1,y_1) \quad (8)$$

caused by rectangular exposure at any evaluation point can be obtained by 2 additions and 2 subtractions.

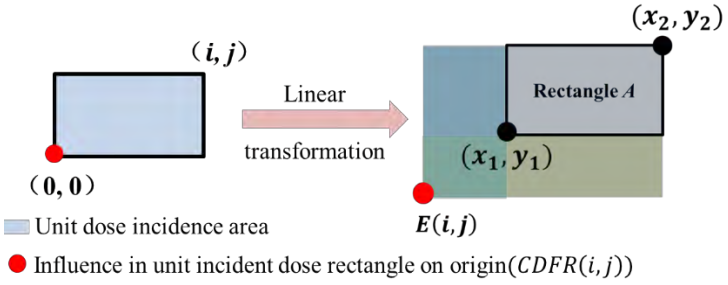

Figure 3. Schematic diagram of calculating energy deposition by CDFR table.

If the CDFR table is in the range of three times α, the table total size is $3\alpha \times 3\alpha$. Suppose that when α=10 nm, the CDFR table size is 9×10^2. Therefore, the memory consumption is small, and the calculation speed is fast.

***Step* (2)** Query rectangles in adjacent region. In Figure 1(b), for evaluation point *O*, its adjacent region is a square region centered on *O* with a side length of 6α. R-tree is used to quickly find the rectangles in the adjacent region[19]. During PE simulation, R-tree structure will not change to achieve efficient insertion and query purposes.

***Step* (3)** Calculate the evaluation point forward-scattering energy deposition intensity. As shown in Figure 1(b), point *O* is the evaluation point, and the rectangle beam spots in the search area all contribute to the forward-scattering energy deposition value of point *O*. Since α is small, the adjacent region is small and the number of rectangles in the adjacent region is small. Thus, the calculation of the forward-scattering energy deposition for each position only needs a few additions and subtractions.

D. Back-scattering calculation

The back-scattering energy deposition simulation method (Figure 1(b)) mainly consists of four steps:

***Step* (1)** Determine the mesh size. The determination of mesh size is based on the back-scattering parameter β and the required calculation accuracy. The proposed method disregards the specific distribution of patterns within the grid. Instead, it only focuses on the overall exposure dose.

***Step* (2)** Calculate the grid area density, i.e., the total exposure dose within the grid. It is the sum of all the grid feature areas multiplied by the corresponding exposure dose. The grid layout area density is

$$D_i = \sum_{j=1}^{n} \sigma_{ij} a_{ij} \quad (9)$$

where D_i represents the layout area density of grid i, n is the number of features in grid i, σ_{ij} is the exposure dose of the j feature in grid i, and a_{ij} represents the area of the j feature related to grid i.

***Step* (3)** Convolve D_i with the PSF. The exposure dose for each grid is concentrated in the center of the grid by default. The time complexity of traditional convolution is $O(N^2)$, where N is the number of grids. While FFT is used to accelerate the convolution calculation which exhibit a time complexity of $O(NlogN)$.

***Step* (4)** Calculate the back-scattering energy deposition. In ***Step* (3)**, the back-scattering energy deposition density at the center of the grid can be obtained, and its value at other positions can be calculated by spline interpolation, which offers high interpolation accuracy.

E. EPE calculation

EPE can be used to describe the accuracy of the PEC calculation results. When EPE meets the layout lithography requirements, the correction calculation can be terminated.

The EPE calculation consists of the following four steps:

***Step* (1)** Place the EPE measuring points. Place the measuring points evenly along the polygon boundary based on the preset parameters. And make sure that the Manhattan polygon vertexes are part of the measuring points.

***Step* (2)** Determine the EPE measurement direction. In the case of underexposure, the EPE measuring point should be directed towards the interior polygon; conversely, in the event of overexposure, the direction should be oriented towards the exterior polygon.

***Step* (3)** Calculate the EPE of the measuring points. According to the measurement direction, the energy deposition density of each point is calculated until it meets the requirements, that is, within the polygon, the energy deposition density should be greater than the developmental threshold, while outside the polygon, the energy deposition density should be less than the developmental threshold.

***Step* (4)** Calculate the average EPE. The formula

$$EPE = \frac{\sum_{i=1}^{N} EPE_i}{N} \tag{1}$$

is used in the calculation, where N is the number of placed measurement points; and EPE_i is the EPE of each position.

3. DATA

In this section, we introduce the data sources of the Manhattan layouts used in the experiment.

The Manhattan layouts used in the experiment are partially taken from prior work of our research group[20]. In addition, we also test part of the open-source Manhattan layouts to demonstrate the robustness of the proposed method. The layouts we tested are published on https://github.com/LiuGroupHNU/PEC3.0.

4. RESULT

In this section, a series of performance tests are carried out on the proposed method from the aspects of calculation accuracy, correction accuracy, time consumption and memory consumption. Unless otherwise noted, all experiments in this section are run on an Intel(R) Xeon(R) CPU E5-2690 v2@3.00 GHz with 10 CPU cores and 64 GB RAM.

A. Accuracy analysis

To validate the accuracy of the proposed forward-/back-scattering separation method in calculating energy deposition, we extend the cumulative influence of adjacent region to the entire layout to calculate the energy deposition density at each position, which is used as the precision measurement basis of the proposed method.

Under the above experimental conditions, Table 1 shows the maximum absolute error and maximum relative error between the energy deposition values calculated by the proposed forward-/back-scattering separation method and the theoretical values. As the mesh size decreases, the accuracy of the proposed method increases, and the accuracy of the pixel-level can be reached.

Table 1. Maximum absolute errors (AE) and maximum relative errors (RE) of PE simulation in different mesh sizes.

mesh sizes	Manhattan layout	
	max (AE)	max (RE)
1 nm	1.67×10^{-5}	2.18×10^{-5}
β/6 (304 nm)	1.58×10^{-4}	2.07×10^{-4}
β/8 (228 nm)	1.10×10^{-4}	1.44×10^{-4}
β/10 (182 nm)	8.36×10^{-5}	1.10×10^{-4}
β/12 (152 nm)	5.37×10^{-5}	7.02×10^{-5}

The incident dose of the EBL system is not continuous. For example, when there are 128 dose levels, the discretization error is about 1/128≈0.78%. The accuracy of the EBL exposure simulation can be compared with the dose error of the lithography machine. Therefore, the mesh size can be selected according to the dose control error of the EBL machine and the CD of the layout to balance the calculation speed and accuracy.

To quantitatively assess the robustness of the proposed PEC method, we test multiple Manhattan layouts in our benchmark calculation. For various Manhattan layouts, the proposed method consistently maintains the EPE below 1 nm after PEC, as shown in Figure 4.

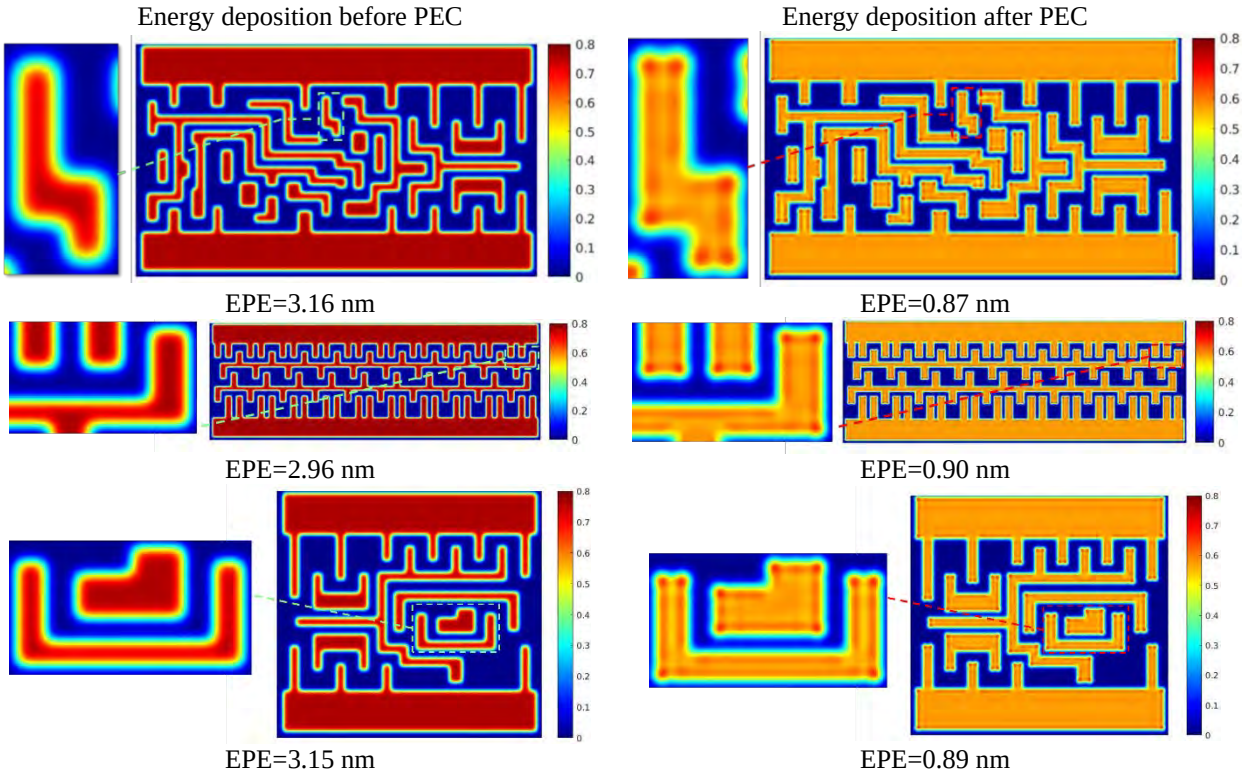

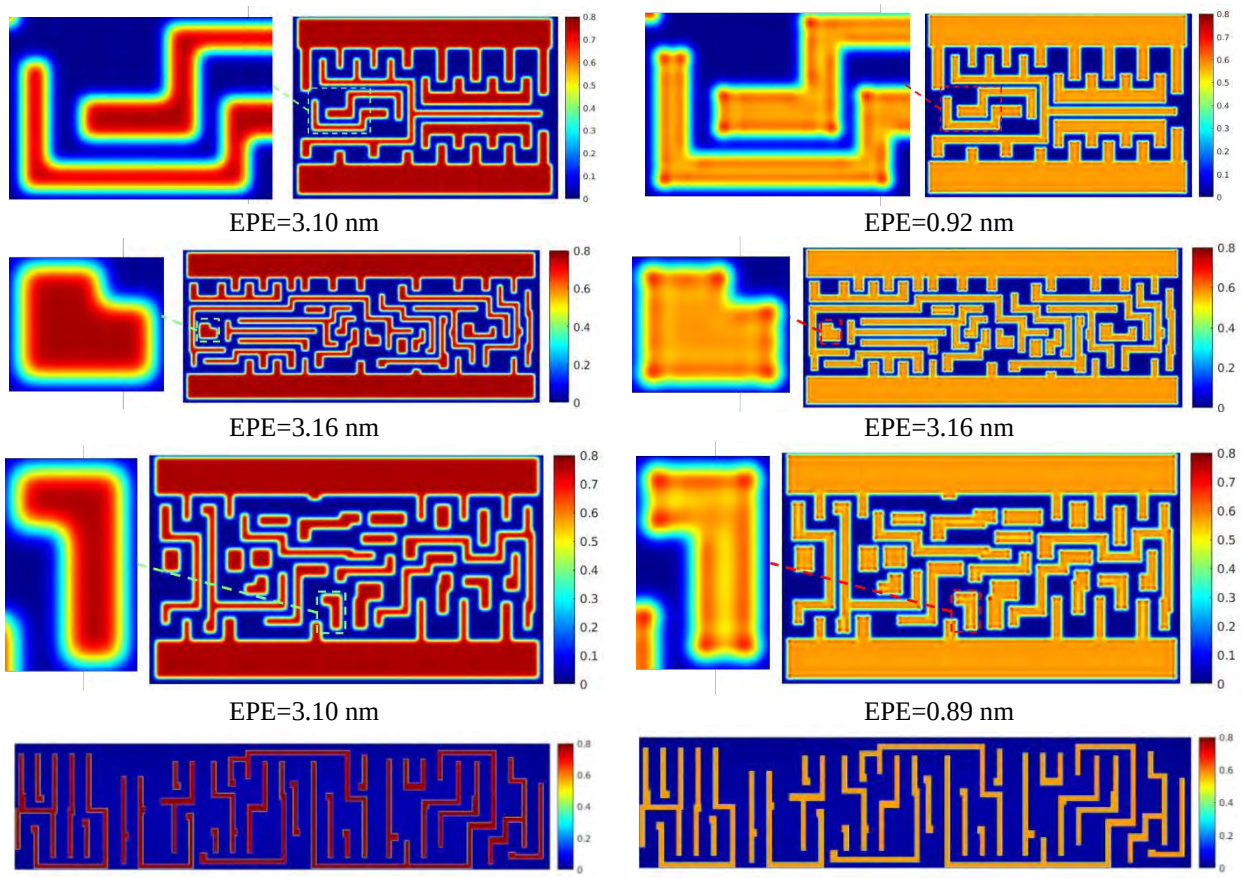

Figure 4. Comparison of energy deposition effects in the experimental layouts before and after PEC.

B. Time consumption

To test the efficiency of the proposed method, multiple test sets on multiple lithographic layouts of different sizes are performed. The forward-/back-scattering simulation time are tested in different layouts (Figure 5(a)). Furthermore, the calculation time of 5 dose correction and 5 shape correction in different layouts is also tested (Figure 5(a)).

It can be found that the time consumption for forward-/back-scattering, dose correction and shape correction varies linearly with the layout size, which indicates that the proposed method has strong scalability.

C. Memory consumption

The spatial complexity of the proposed method is $O(N)$, where N represents the number of rectangle beam spots after layout fracturing. We evaluate the memory consumption of the proposed method across various layout sizes (Figure 5(b)). The experiments demonstrate that the memory consumption varies linearly with the layout size.

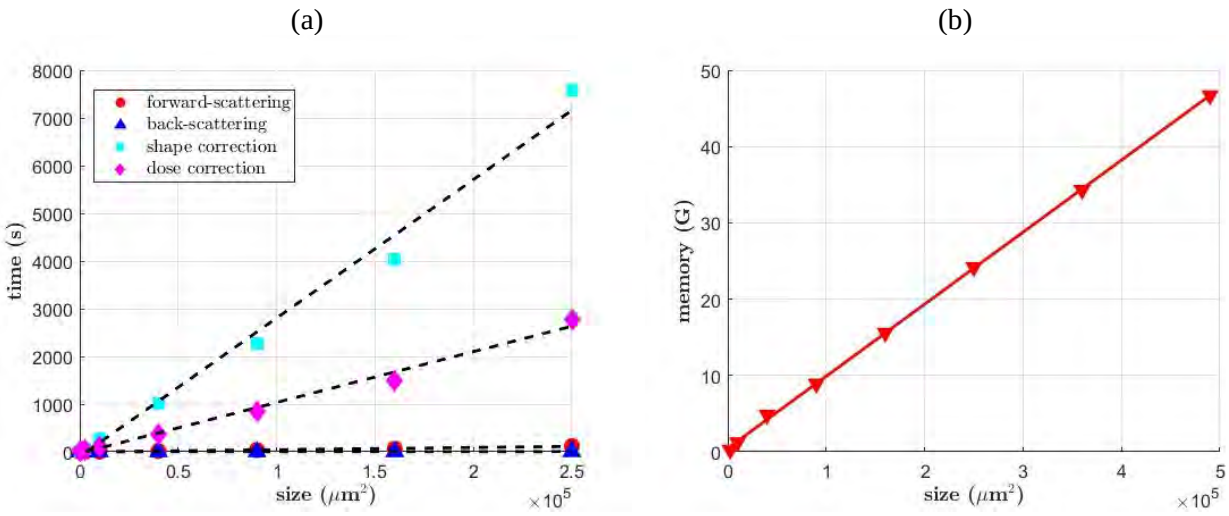

Figure 5. (a) The time consumption for forward-/back-scattering and shape/dose correction varying with layout size. (b) The memory consumption varying with layout size.

5. CONCLUSIONS

In this paper, a hybrid PEC method based on separation of forward-/back-scattering and CDF is proposed, which overcomes the limitation of memory and time. The calculation results in our experimental benchmarks show that both the time consumption and the memory consumption of the proposed method vary linearly with the layout size. Compared to the traditional pixel-level PEC method, the modeling efficiency of the proposed method can be improved by about 3 orders of magnitude. The proposed method might be useful in large-scale mask data preparation (MDP) and direct-write EBL applications.

ACKNOWLEDGEMENTS

This work is supported by the Yuelushan Center for Industrial Innovation (2023YCII0104); the National Natural Science Foundation of China (61804049); the Huxiang High Level Talent Gathering Project (2019RS1023); the Technology Innovation and Entrepreneurship Funds of Hunan Province, P.R. China (2019GK5029); the Fund for Distinguished Young Scholars of Changsha (kq1905012); the National Natural Science Foundation of China (62101182); the Fundamental Research Funds for the Central Universities of P.R. China.

REFERENCES

[1] CHANG T. Proximity effect in electron-beam lithography [J]. Journal of vacuum science and technology, 1975, 12(6): 1271-5.

[2] ERIKSEN E H, NAZIR A, BALLING P, et al. Dose regularization via filtering and projection: An open-source code for optimization-based proximity-effect-correction for nanoscale lithography [J]. MICROELECTRONIC ENGINEERING, 2018, 199: 52-7.

[3] PARIKH M. Self-consistent proximity effect correction technique for resist exposure (SPECTRE) [J]. Journal of vacuum science and technology, 1978, 15(3): 931-3.

[4] ABE T, YAMASAKI S, YOSHIKAWA R Y R, et al. Representative figure method for proximity effect correction [J]. Japanese journal of applied physics, 1991, 30(3B): L528.

[5] ABE T, YAMASAKI S, YAMAGUCHI T, et al. Representative Figure Method for Proximity Effect Correction [II] [J]. Japanese Journal of Applied Physics, 1991, 30(11R): 2965.

[6] ABE T, YAMASAKI S, YOSHIKAWA R, et al. The representative figure method for the proximity effect correction [III] [J]. Journal of Vacuum Science & Technology B: Microelectronics and Nanometer Structures Processing, Measurement, and Phenomena, 1991, 9(6): 3059-62.
[7] HOU C, YAO W, LIU W, et al. Ultrafast and accurate proximity effect correction of large-scale electron beam lithography based on FMM and saaS; proceedings of the 2020 International Workshop on Advanced Patterning Solutions (IWAPS), F, 2020 [C]. IEEE.
[8] LIU W, YAO W, HOU C, et al. HNU-EBL: A Software Toolkit for Electron Beam Lithography Simulation and Optimization; proceedings of the 2021 International Workshop on Advanced Patterning Solutions (IWAPS), F, 2021 [C]. IEEE.
[9] ZHAO H, YAO W, XU H, et al. Accurate and Efficient Proximity Effect Correction for Electron Beam Lithography Based on Distributed Parallel Computing; proceedings of the 2022 International Workshop on Advanced Patterning Solutions (IWAPS), F, 2022 [C]. IEEE.
[10] YAO W, ZHAO H, HOU C, et al. Efficient Proximity Effect Correction Using Fast Multipole Method with Unequally Spaced Grid for Electron Beam Lithography [J]. IEEE Transactions on Computer-Aided Design of Integrated Circuits and Systems, 2022.
[11] KLIMPEL T, SCHULZ M, ZIMMERMANN R, et al. Model based hybrid proximity effect correction scheme combining dose modulation and shape adjustments [J]. Journal of Vacuum Science & Technology B, 2011, 29(6): 06F315.
[12] FRANZBLAU D S. Performance guarantees on a sweep-line heuristic for covering rectilinear polygons with rectangles [J]. SIAM journal on discrete mathematics, 1989, 2(3): 307-21.
[13] TSUNODA D, SHOJI M, TSUNOE H. Proximity effect correction concerning forward scattering; proceedings of the Photomask Technology 2010, F, 2010 [C]. SPIE.
[14] MURAI F, YODA H, OKAZAKI S, et al. Fast proximity effect correction method using a pattern area density map [J]. Journal of Vacuum Science & Technology B: Microelectronics and Nanometer Structures Processing, Measurement, and Phenomena, 1992, 10(6): 3072-6.
[15] ABE T, HATTORI Y, IIJIMA T, et al. High-accuracy proximity effect correction for mask writing [J]. Japanese Journal of Applied Physics, 2007, 46(2R): 826.
[16] LEE S-Y, COOK B D. PYRAMID-a hierarchical, rule-based approach toward proximity effect correction. I. Exposure estimation [J]. IEEE Transactions on Semiconductor Manufacturing, 1998, 11(1): 108-16.
[17] LEE S-Y, HU F, JI J. Representation of nonrectangular features for exposure estimation and proximity effect correction in electron-beam lithography [J]. Journal of Vacuum Science & Technology B: Microelectronics and Nanometer Structures Processing, Measurement, and Phenomena, 2004, 22(6): 2929-35.
[18] LEE S Y. A flexible and efficient approach to E‐beam proximity effect correction—PYRAMID [J]. Surface and Interface Analysis: An International Journal devoted to the development and application of techniques for the analysis of surfaces, interfaces and thin films, 2005, 37(11): 919-26.
[19] CHEUNG K L, FU A W-C. Enhanced nearest neighbour search on the R-tree [J]. ACM SIGMOD Record, 1998, 27(3): 16-21.
[20] ZHAO Z, TAN Z, MO P, et al. A Heterogeneous Parallel Non-von Neumann Architecture System for Accurate and Efficient Machine Learning Molecular Dynamics [J]. IEEE Transactions on Circuits and Systems I: Regular Papers, 2023.